

## Eco-valorification of marine shells by hydrothermal conversion in alkaline media

A. Bucur<sup>a</sup>, R. Banica<sup>a</sup>, M. C. Pascariu<sup>a</sup>, M. Poienar<sup>a</sup>, C. Mosoarca<sup>a,\*</sup>, R. Bucur<sup>a</sup>,  
A. Negrea<sup>a,b</sup>, I. Hulka<sup>c</sup>

<sup>a</sup>Renewable Energy and Electrochemistry Department, National Institute of R&D for Electrochemistry and Condensed Matter - INCEMC, 144 Aurel Păunescu-Podeanu, RO-300569, Timișoara, Romania

<sup>b</sup>Faculty of Industrial Chemistry and Environmental Engineering Politehnica University of Timisoara 6 Vasile Pârvan Blvd., RO-300223 Timișoara, Romania,

<sup>c</sup>Research Institute for Renewable Energy - ICER Politehnica University of Timisoara 138 Gavril Musicescu, RO-307221, Timișoara, Romania

Marine shells are a natural, cheap, abundant and renewable resource, which can be used to produce useful materials, such as for the construction industry. The present study focuses on the transformation of *Mya arenaria* exoskeletons from the Black Sea into calcium hydroxide by using low-temperature hydrothermal synthesis. In contrast with other methods, this energy-saving process does not involve calcination of shells prior to the hydrothermal treatment. XRD results show the formation of calcium hydroxide with preferential orientation and interesting atypical morphology, which is strongly influenced by the composition of the reaction medium.

(Received October 10, 2021; Accepted February 2, 2022)

**Keywords:** Hydrothermal synthesis, Materials sciences, Calcium, Renewable resources, Sustainable chemistry

### 1. Introduction

Marine shell waste contributes to vital environmental issues because of off-odor and concentration of minerals in landfills. About 25% (over twenty million tons) of the whole weight of annual marine production is discarded as waste [1], which is commonly disposed in landfills, processed into feed stock or used as plant fertilizers. Landfilling of waste shells can cause several environmental problems like generation of odours, contamination of air, soil pollution and harm the marine environment [2].

There is a great potential for conversion of this waste into products in order to solve some of the problems associated with pollution and disposal. Shells account for a major proportion of food process waste that is not being widely used and thus provides significant opportunities for development of added-value products. As a result, the interest in the conversion and utilization of these waste materials has grown [3], such as for poultry food supplements [4, 5], farm cows' food supplements [6] or rats' diet supplement [7]. The high content of calcium carbonate in clamshell waste may be used as an alternate material for the hydroxyapatite (HA) production, with a number of advantages [8].

Calcium hydroxide is a material widely used in the constructions industry, representing a major component of lime mortar, hydrated cement and having a wide range of other applications [9,10]. It is usually obtained in industry from natural limestone. In the first step the minerals have to be mined, while the second step requires the conversion of limestone into calcium oxide. The second step is energy consuming ( $\Delta H = +3010$  kJ/kg at 900 °C) and takes place at high temperatures (~900 °C for complete calcination) [11]. A sustainable alternative involves the production of calcium hydroxide from organic wastes which contain calcium carbonate, such as seashells. First, calcium oxide is obtained through thermal treatment close to 900 °C, followed by the reaction with water [12] or other chemicals, such as hydrochloric acid and sodium hydroxide

---

\* Corresponding author: m.cristina@gmail.com  
<https://doi.org/10.15251/DJNB.2022.171.153>

[13,14]. Hydrothermal treatment has also been successfully employed in the production of this material. Calcium hydroxide and hydroxyapatite have been reported as constituents of the reaction product obtained by a combination of calcination at high temperatures and hydrothermal processing at low temperature, using cockle shells [15].

We propose a more economically viable method for obtaining calcium hydroxide, which involves much lower temperatures, lower energy consumption rates and the use of renewable resources, namely sea shells. In this study we directly converted aragonite from sea shells exoskeletons (*Mya arenaria* species) into calcium hydroxide by hydrothermal synthesis at low temperature and pressure, without prior calcination. The reaction product does not contain other crystalline phases with the exception of the crystalline polymorphs existing in shells. The presence of sodium hydroxide alone or in combination with sodium sulfite influences the morphology and crystallization of calcium hydroxide. To our knowledge, there is no study reported in the literature about the direct achievement of calcium hydroxide by hydrothermal means, without calcination of shells prior to the hydrothermal treatment. This approach can find applications as a means to directly convert shells into crystalline calcium hydroxide in a low energy-consuming process, and represents an ecological way to integrate shells waste into the production of low-cost materials.

## 2. Experimental

### 2.1. Identification

A number of mollusc shells were collected from the Black Sea shore and examined to determine their species. *Mya arenaria*, presented in Figure 1a, was chosen for this study.

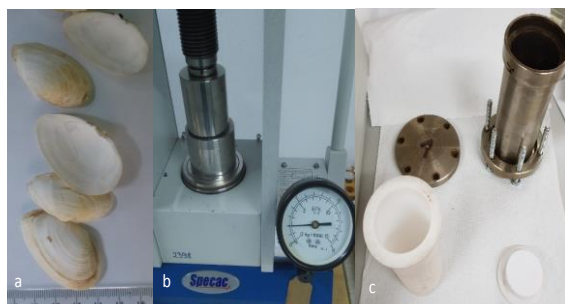


Fig. 1. a. *Mya arenaria* shells; b. Hydraulic press used for shells processing; c. Teflon liner (bottom) and metal autoclave (top).

### 2.2. Processing

The shells were washed for a number of times in distilled water under ultrasonic treatment, followed by drying for 2 hours at 80 °C. Then the shells were broken, one by one, by pressing them between 2 steel cylinders with a diameter of about 50 mm for 30 seconds, using the hydraulic press (presented in Figure 1b). At the end of the above-mentioned steps, the resulting fragments were sieved through meshes of different sizes and collected for further processing and characterizations. In order to analyse the structural, morphological and thermal behaviour of the hydrothermally treated *Mya arenaria* shells, the fraction 0.3-0.8 mm was chosen for this study.

Table 1. Reagents used in the hydrothermal experiments

Sample name	NaOH conc. [mol L <sup>-1</sup> ]	Na <sub>2</sub> SO <sub>3</sub> conc. [mmol L <sup>-1</sup> ]
F1	0	0
SC1	3	0
SC2	3	2
SC3	3	8

### 2.3. Hydrothermal processing

Certain amounts (100 mg) of shells specimens were weighted and inserted into Teflon liners and metal autoclaves (Figure 1c). Afterwards, 20 mL of the reagents listed in Table 1 were added. The autoclaves were heated at 140 °C for 20 h, then naturally cooled to room temperature. The treated shells were washed 4-5 times with small amounts of distilled water, then dried in the oven at 70 °C for 2 h. F1 represents the raw shells sample, which was not subjected to hydrothermal treatment.

### 2.4. Physico-chemical characterization

X-ray powder diffraction (XRD) patterns were obtained using an X'Pert PRO MPD diffractometer with PixCEL detector and copper anode ( $\lambda=1.540598$  Å), on zero background silicone rotating holders. The structural characterization was performed using a scanning electron microscope (Quanta 250 FEG), coupled with an EDX detector for the semi-quantitative analysis of shell samples. Thermal stability was studied using the SETARAM Lab Sys Evo equipment. The powder is placed in an alumina crucible and heated with 15 deg min<sup>-1</sup> heating rate in synthetic air (42 mL min<sup>-1</sup>), up to 1000 °C

## 3. Results and Discussions

XRD results show that the sample containing raw shells (sample F1) is single phase, well crystallized within the aragonite type (polymorph of CaCO<sub>3</sub> encountered in shells structure). The ICDD file used for analysis is 00-041-1475. As can be observed in Figure 2, all peaks are sharp and well defined, with no other crystalline phase present.

Hydrothermally treated samples SC1, SC2 and SC3 contain Ca(OH)<sub>2</sub> which is the predominant phase (91-93%, as determined by HighScore Software), and small amounts of calcite and aragonite, phases which are polymorphs of CaCO<sub>3</sub> encountered in the shells composition. Identification made use of the ICDD file mentioned for aragonite, 01-072-1937 for calcite and 01-081-2040 for calcium hydroxide. The peaks of sample SC1 are very intense and sharp, indicating large crystalline domains; this sample presents a strong preferential orientation growth of calcium hydroxide phase along the (001) crystallographic direction. The same shape and high intensity of peaks is encountered in the SC2 sample, but the addition of Na<sub>2</sub>SO<sub>3</sub> led to the increase of the intensity of the (101) peak, reducing the preferential growth effect. This reagent breaks down disulfide bonds existing between the aragonite layers of the shells, transforming each of these bridges into two S-sulfonate groups, so the chemical crosslinking in proteins that compose the organic layers in seashells can be reduced [16, 17]. This allows for a more efficient access of the hydroxide ion to the aragonite surfaces, so the reaction rate should increase, which explains the inhibition of the preferential growth.

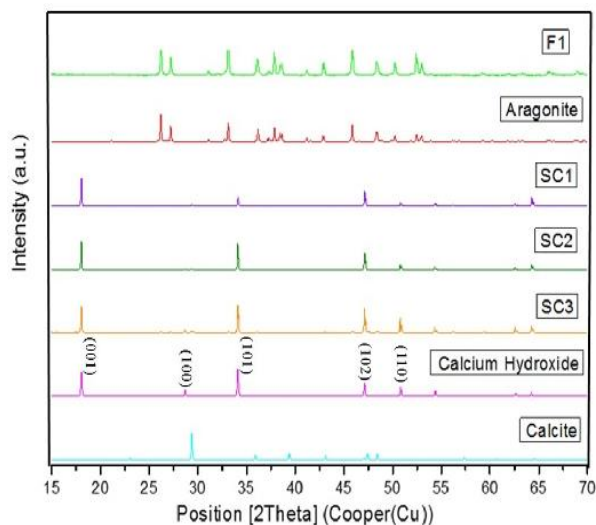
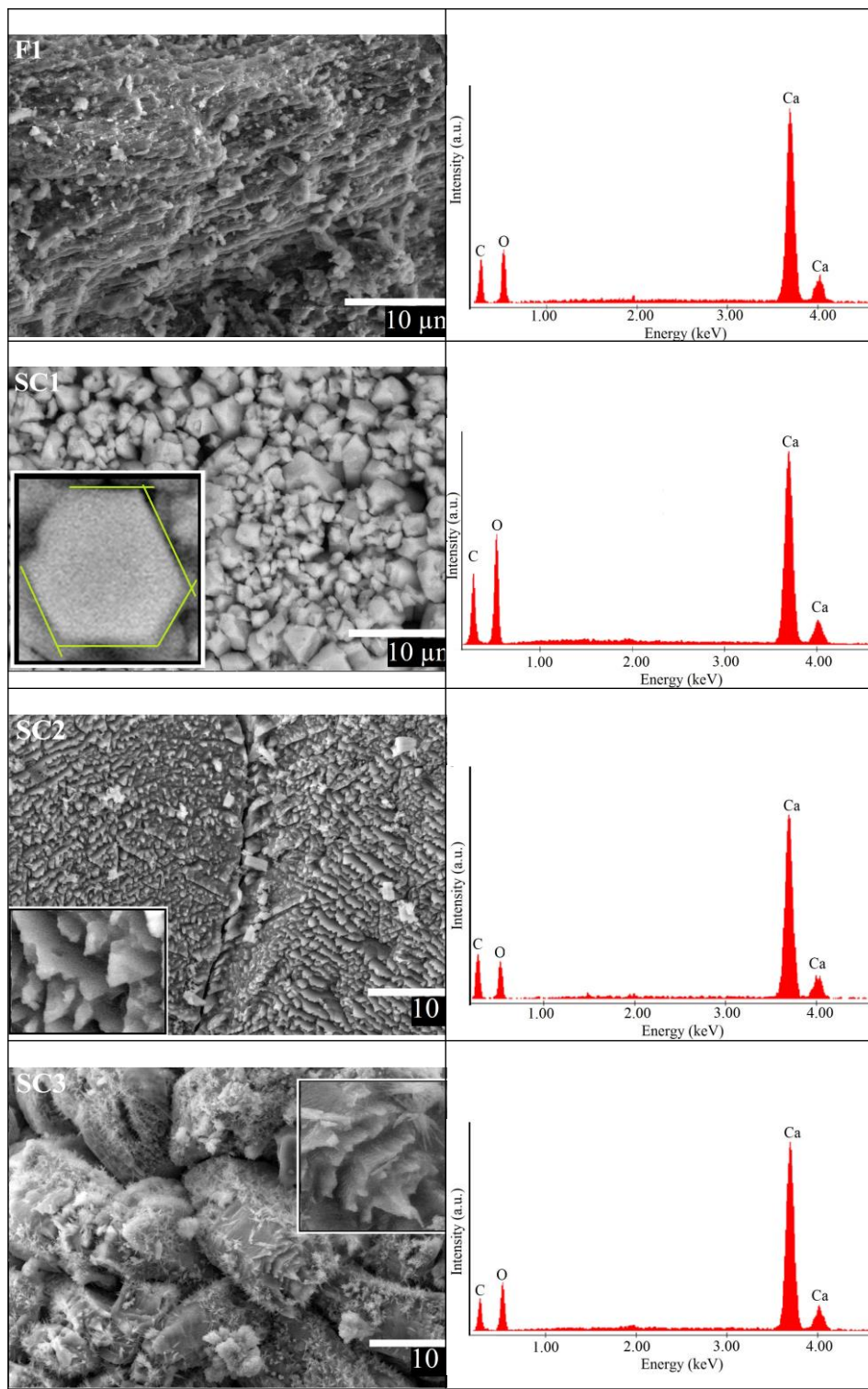


Fig. 2. XRD patterns of raw shells (F1) and samples hydrothermally treated with solutions from Table 1 (SC1÷3). Aragonite, calcite and calcium hydroxide represent standard patterns.

Addition of  $\text{Na}_2\text{SO}_3$  in a higher amount in the sample SC3 led to the crystallization of calcium hydroxide in agreement with the standard profile of the pattern of this material. The growth along the (001) direction decreases from SC2 to SC3, while the intensity of the (101) peak grows from SC1 to SC2 and remains the same from SC2 to SC3. There is no change in the crystallinity degree from sample SC2 to sample SC3, but the obvious effect of lowering the preferential growth effect.

The semi-quantitative analysis by EDX identified the presence of Ca, C and O, as can be seen in Figure 3. The SEM image of sample F1 (Figure 3) presents a typical structure of layers, characteristic for the shells [18]. Sample SC1, even if composed mostly of calcium hydroxide, presents a structure which is not typical for this material, which usually adopts a platy hexagonal habit [13,14,19, 20]. The particles are in the shape of blocks, with a dimensional distribution in the range of 1-10  $\mu\text{m}$  and with non-uniform contours. 60 and 120 degrees angles can be observed for some of the particles (inset in Figure 3), which evidence the hexagonal crystallization of calcium hydroxide (in agreement with XRD results). Even if the standard morphology is that of hexagonal lamellae, a strong preferential crystalline growth along the (001) direction exists in the case of sample SC1 (according to XRD), which takes the form of hexagonal prisms.



*Fig. 3. SEM images of raw shells (F1) and of the three samples obtained by hydrothermal treatment, and the corresponding EDX patterns.*

When a small amount of  $\text{Na}_2\text{SO}_3$  was added to the synthesis, the morphology changed considerably (sample SC2): an ordered array of lamellae is visible, with endings growing as if they are melted and then cooled down. This lamellar structure resembles mostly the original shells appearance. The growth of calcium hydroxide takes place presumably at the edges of aragonite

lamellae (using Ca ions as precursors); these edges start forming 60 degrees-angles and sometimes they turn into triangular prisms (inset in Figure 3).

Increasing the amount of  $\text{Na}_2\text{SO}_3$  led to a new surprising change of morphology (sample SC3): big irregularly shaped blocks forming macles, covered with a fine layer of blade-like crystals, grouped in the shape of stars. Layers of parallel crystals are slightly visible, perpendicular to the main direction of the largest formations, which have the appearance of rolled sheets of paper. With the exception of sample SC1, which is in the form of granules in the micrometric size, all the samples are composed of big blocks.

Thermogravimetric analysis for the first sample (F1) is presented in Figure 4 (top). The XRD analysis indicates that the sample crystallized in aragonite structure, without any secondary phases as stated before (Figure 2). A small endothermic peak at 315 °C in the heat flow curve is determined by the conversion of aragonite into calcite [21]. A large weight loss of approximately 41% is observed between 600 and 820 °C and is associated with thermal decomposition of  $\text{CaCO}_3$  to  $\text{CaO}$ , as mentioned in literature [22]. From the TG analysis of samples SC1, SC2 and SC3 it can be observed that a slightly different thermal behaviour occurred in particular in the case of SC2 and this could be associated with the different percentages of phases in each sample:  $\text{Ca}(\text{OH})_2$  main phase and aragonite/calcite as minor phases, as indicated by XRD analysis. The first weight loss begins at approximately 400 °C (19.5 % for SC1, 16.6 % for SC2 and 21.79 % for SC3, respectively), corresponding to the dehydration of the calcium hydroxide to  $\text{CaO}$ . A second weight loss step is observed for each sample starting from approximately 600 °C and reaching the final plateau at ~ 780 °C, corresponding to the decomposition of  $\text{CaCO}_3$  to  $\text{CaO}$ . There are small differences, though, for this temperature interval, more pronounced for SC2 sample. These differences are most likely determined by the size of  $\text{CaCO}_3$  particles [19].

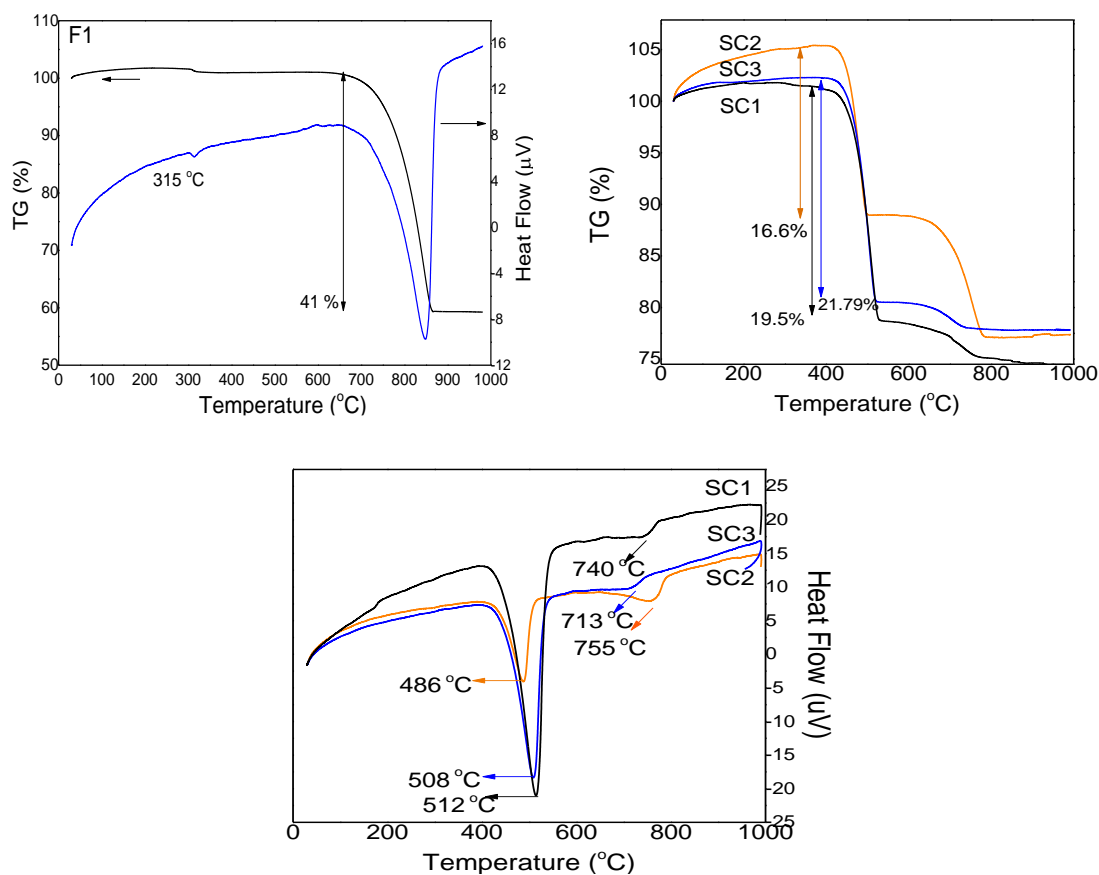


Fig. 4. Top: TG analysis for F1 sample in air from RT to 1000 °C (Heat Flow curve - right axis); bottom: TG analysis for SC1, SC2 and SC3 samples in air from RT to 1000 °C (left) and Heat Flow curves for SC1, SC2 and SC3 samples (right).



Two endothermic peaks are associated with these thermal decompositions in the heat flow curves, a high intensity one at 512 °C for SC1, 486 °C for SC2 and 508 °C for SC3 – due to the decomposition of Ca(OH)<sub>2</sub> to CaO, and a small intensity peak at 740 °C for SC1, 755 °C for SC2 and 713 °C for SC3, due to the decomposition of CaCO<sub>3</sub> to CaO (Figure 4 bottom - right).

#### 4. Conclusions

The hydrothermal synthesis was used to directly convert aragonite from sea shells exoskeletons (*Mya arenaria*) into calcium hydroxide, without the use of extreme conditions or high energy requirement. The hydrothermal synthesis in the presence of NaOH led to the formation of Ca(OH)<sub>2</sub> with strong preferential orientation, while the presence of Na<sub>2</sub>SO<sub>3</sub> coupled with NaOH led to the formation of Ca(OH)<sub>2</sub> with different morphologies, and the decrease of the preferential orientation growth with the increase in the amount of sulphite content. Considering the numerous applications of Ca(OH)<sub>2</sub>, the properties of these morphological modifications are to be explored for new directions of study and usage.

#### Acknowledgements

This work was supported by a grant of the Romanian Ministry of Education and Research, CNCS - UEFISCDI, project number PN-III-P1-1.1-TE-2019-2116, within PNCDI III.

#### References

- [1] A. Malik, E. Grohmann, Environmental protection strategies for sustainable development, Springer Nature Switzerland AG, (2011).; <https://doi.org/10.1007/978-94-007-1591-2>
- [2] J. H. Jung , J. J. Lee , G. W. Lee , K. S. Yoo, B. H. Shon, Achilias D. Material recycling - trends and perspectives, IntechOpen Limited London, (2012).
- [3] Y. Hou, A. Shavandi, A. Carne, A. A. Bekhit, T. B. Ng, R. C. F. Cheung, A. El-din A. Bekhit, Crit. Rev. Env. Sci. Tec. 46(11-12), 1047 (2016); <https://doi.org/10.1080/10643389.2016.1202669>
- [4] A. O. Oso, A. A. Idowu, O. T. Niameh, J. Anim. Physiol. Anim. Nutr. 95, 461 (2011); <https://doi.org/10.1111/j.1439-0396.2010.01073.x>
- [5] F. V. Muir , P. C. Harris , R. W. Gerry, Poult Sci. 55, 1046 (1976); <https://doi.org/10.3382/ps.0551046>
- [6] A. D. Finkelstein, J. E. Wohlt, S. M. Emanuele, S. M. Tweed, J. Dairy. Sci. 76(2), 582 (1993); [https://doi.org/10.3168/jds.S0022-0302\(93\)77378-6](https://doi.org/10.3168/jds.S0022-0302(93)77378-6)
- [7] M. Shono, I. Shimizu, E. Aoyagi, T. Taniguchi, H. Takenaka, M. Ishikawa, M. Urata, K. Sannomiya, K. Tamaki, N. Harada, Y. Nakaya, T. Takayama, Biosci. Biotechnol. Biochem. 72(10), 2761 (2008); <https://doi.org/10.1271/bbb.80267>
- [8] D. F. Fitriyana, R. Ismail, Y. I. Santosa, S. Nugroho, A. J. Hakim, M. Syahreza Al Mulqi, International Biomedical Instrumentation and Technology Conference (IBITeC) Indonesia, 23 - 24 October, 7-11, (2019).
- [9] R. Graves, J. Eades, L. Smith in Innovations and Uses for Lime, ed. D. Walker, T. Hardy, D. Hoffman, D. Stanley, West Conshohocken PA, 65 (1992).
- [10] H. G. Midgley, Cem Concr Res. 9, 77 (1979); [https://doi.org/10.1016/0008-8846\(79\)90097-8](https://doi.org/10.1016/0008-8846(79)90097-8)
- [11] V. C. H. Wiley, in Ullmann's Encyclopedia of Industrial Chemistry, Seventh Edition, Wiley VCH Verlag GmbH & Co, (2011).
- [12] S. Santhosh, P. S. Balasivanandha, Int. J. Biomed. Nanosci. Nanotechnol. 2(3/4), 276 (2012).
- [13] M. D. Khan, J. W. Ahn, G. Nam, J. Environ. Manage. 223, 947 (2018); <https://doi.org/10.1016/j.jenvman.2018.07.011>

- [14] M. D. Khan , T. Chottititupawong , H. H. T. Vu , J. W. Ahn, G. M. Kim, ACS Omega 5(21), 12290 (2020); <https://doi.org/10.1021/acsomega.0c00993>
- [15] N. A. S. Mohd Puad, L. T. Chuan, N. S. Salman, M. A. Selimin, A. F. A. Latif, M. S. Muhamad, H. Z. Abdullah, M. I. Idris, S. N. H. Mustapha, Biointerface Res. Appl. Chem. 10(4), 5787 (2020); <https://doi.org/10.33263/BRIAC104.787791>
- [16] L. J. Bailey, D. R. Cole, J. Biol. Chem. 234(7), 1733 (1959); [https://doi.org/10.1016/S0021-9258\(18\)69917-X](https://doi.org/10.1016/S0021-9258(18)69917-X)
- [17] M. Schmid, T. K. Prinz, A. Stabler, S. Sangerlaub, Front. Chem. 4(49), 1 (2017); <https://doi.org/10.3389/fchem.2016.00049>
- [18] F. Marin, N. Le Roy, B. Marie, Front. Biosci. S 4, 1099 (2012); <https://doi.org/10.2741/s321>
- [19] Z. Mirghiasi, F. Bakhtiari, E. Darezereshki, E. Esmaeilzadeh, J. Ind. Eng. Chem. 20, 113 (2014); <https://doi.org/10.1016/j.jiec.2013.04.018>
- [20] C. Rodriguez-Navarro, A. Burgos-Cara, F. Di Lorenzo, E. Ruiz-Agudo, K. Elert, Cryst. Growth Des. 20(7), 4418 (2020); <https://doi.org/10.1021/acs.cgd.0c00241>
- [21] S. Yoshioka, Y. Kitano, Geochem. J. 19, 245 (1985); <https://doi.org/10.2343/geochemj.19.245>
- [22] L. Wang, I. Sondi, E. Matijevic, J. Colloid. Interface. Sci. 218, 545 (1999); <https://doi.org/10.1006/jcis.1999.6463>